Solar Cells, *21* (1987) 313 - 327

MEASUREMENT OF PHOTOVOLTAIC DEVICE CURRENT AS A FUNCTION OF VOLTAGE, TEMPERATURE, INTENSITY AND SPECTRUM*

KEITH EMERY and CARL OSTERWALD

Solar Energy Research Institute, 1617 Cole Boulevard, Golden, CO 80401 (U.S.A.)

(Received May 1986; accepted July 3, 1986)

Summary

A review of measurements of the current *vs.* voltage, temperature, intensity and spectrum in photovoltaic (PV) devices is presented. The relative merits of manual *vs.* automated and research *vs.* production current–voltage and current–wavelength (spectral response) instrumentation are discussed. A summary of contacting methods and artifacts associated with current–voltage measurements is presented.

For the PV conversion efficiency to have meaning, it must be given with reference to a specific intensity, spectrum, temperature and PV area definition. Consensus standards exist for the efficiency measurements, although discrepancies in standard test conditions and area definitions are prevalent in the PV community. A set of procedures for measuring the PV efficiency with respect to a given set of reference conditions is presented together with a brief summary of other performance rating methods.

1. Introduction

The evaluation and assessment of the performance of photovoltaic (PV) devices, modules and arrays in terms of measurable parameters requires the measurement of the current as a function of voltage, temperature, intensity and spectrum. Most noticeable of these parameters is the PV conversion efficiency η, defined as the maximum electrical power P_{max} produced by the PV device(s) divided by the incident photon power P_{in}, which is measured with respect to standard reporting conditions defined by a spectrum, intensity, temperature and area definition. In this paper the mechanisms are described which affect the repeatability and accuracy with which P_{max} is measured. These mechanisms include the measurement technique, contacting method, distributed resistance of the metallization, temperature and intensity.

*Paper presented at the 7th Photovoltaic Advanced Research and Development Project Review Meeting, Denver, CO, U.S.A., May 13, 1986.

0379-6787/87/$3.50 © Elsevier Sequoia/Printed in The Netherlands

The open-circuit voltage V_{oc}, short-circuit current I_{sc} and fill factor ($FF = P_{max}/V_{oc}I_{sc}$) are obtained from illuminated current–voltage (I–V) measurements. Other parameters which can be obtained from I–V measurements are the reverse-bias breakdown voltage, the slope of the characteristic curve at V_{oc} and I_{sc}, and the series and shunt resistances. These parameters, together with their dependences on intensity and temperature, are useful in determining the performance of a device, module or array. The current conduction mechanisms of a device can be inferred from dark I–V or illuminated I–V measurements at different temperatures. If I_{sc} is measured at different monochromatic wavelengths and the light intensity incident on the device is measured, then the spectral response and external quantum efficiency can be determined. The white light intensity voltage bias, monochromatic light intensity and chopping frequency, temperature, electrically active area and spatial non-uniformities in the photoresponse all affect the spectral response.

For PV devices exhibiting slow response times, the measurement of the steady state I–V characteristics is complicated by the constraint that the bias rate of the test system should not drive the device out of the steady state. The contacting to a PV device without ribbons or wires is perhaps the most difficult and operator-dependent part of I–V measurements. The contact area, distributed resistance, contact material and the contact pressure can affect the measurement of P_{max}, FF and η.

2. Photovoltaic performance rating

The performance of a PV device, module or array can be evaluated with respect to its peak power P_{max} or efficiency under a set of test conditions or with respect to the energy produced over a period of time. Various rating methods used by the PV community are summarized in ref. 1 and Table 1.

TABLE 1

Standard reporting conditions for photovoltaic devices, modules and arrays

Application	*Intensity* ($W\ m^{-2}$)	*Spectrum*	*Temperature* (°C)
Terrestrial	1000	ASTM E892 global	25
Concentration terrestrial	>1000	ASTM E891 direct	28
Space	1353, 1372, 1366	AM 0	28
NOCT terrestrial	800	ASTM E892 global	20 °C air temperature, 1 $m\ s^{-1}$ wind velocity

2.1. Efficiency

The PV conversion efficiency η is defined as 100 times P_{max} divided by the incident power under standard reference conditions (intensity, spectrum, temperature and area definition). The currently accepted standard reference conditions for terrestrial efficiency measurements are given in Table 1, row 1.

Various area definitions used by the PV community are summarized in ref. 2. The area definitions for non-concentrator cells state that the entire area of the cell, including the area covered by grids and contacts, should be used. For concentrator cells, the test cell area is the area designed to be illuminated. For modules, the entire frontal area including borders, frame and any protruding lugs should be used. For many of the thin film material systems, the contact area on the substrate is not included because this area is ill defined and would result in unrealistically low efficiencies (less than 1% for the best devices). However, many schemes of raising the fill factor for these thin film cells by bordering the cell with thick silver paste are being employed even in the best devices. A further deviation from the standard cell area definition is used for amorphous silicon cells on glass where the junction covers a large fraction of the substrate, and the cell area used is a small aluminum contact (less than 1 cm^2) deposited onto the p layer. Thin film module efficiencies have also been reported where the active area was used or the border and frame area was neglected.

The incident power for efficiency measurements is normally calibrated using a reference cell whose short-circuit current is calibrated with respect to a tabular reference spectrum. The most accurate method of calibrating a reference cell is to use the following equation [3 - 5]

$$\mathrm{CN} = \frac{I_{sc}^{R,S}}{E_{tot}} \frac{\int E_R(\lambda)\mathrm{SR}_R(\lambda)\,d\lambda \int E_S(\lambda)\,d\lambda}{\int E_R(\lambda)\,d\lambda \int E_S(\lambda)\mathrm{SR}_R(\lambda)\,d\lambda} \quad (1)$$

CN is known as the calibration number for a given reference cell and when multiplied by 1000 W m^{-2} gives the short-circuit current of the reference cell under the normalized reference spectrum. The short-circuit current $I_{sc}^{R,S}$ of the reference cell, the total irradiance E_{tot} and the relative solar spectral irradiance $E_S(\lambda)$ are measured at the same time with the same field of view. The relative spectral response is $\mathrm{SR}_R(\lambda)$.

The term air mass (AM) in the context of eqn. (1) is almost meaningless since a reference cell is not calibrated with respect to an AM 0 or AM 1.5 spectrum, but with respect to an arbitrary tabular spectrum $E_R(\lambda)$. Figure 1 further shows that the term AM has almost no meaning in the context of PV efficiency measurements, since almost any spectrum or intensity can be obtained at AM 1.5. A comparison of the differences in CN (eqn. (1)) for different published AM 1.5 and AM 0 spectra is given in Figs. 2 and 3 for various cell technologies (Fig. 4). Figure 2 shows a 12% spread in the calibration number depending on the cell technology and reference spectrum. As shown in Fig. 2(a), crystalline silicon is relatively insensitive to the choice of AM 1.5 reference spectra. The calibration number for low

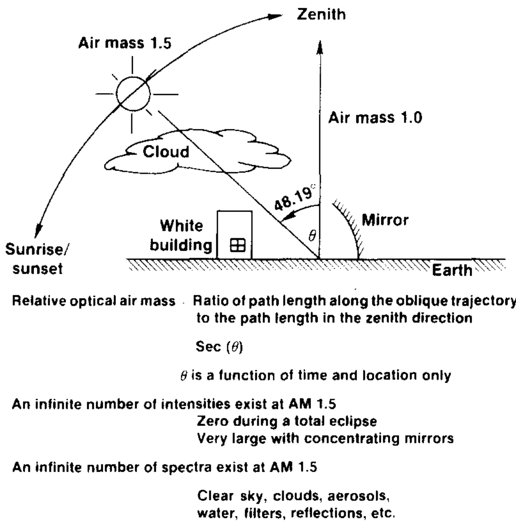

Fig. 1. Graphical description of the relative optical AM.

band gap material systems ($CdS/CuInSe_2$) is lower for global reference spectra than it is for direct reference spectra, whereas the opposite is true for high band gap material systems (amorphous silicon, GaAlAs, GaAsP). The same atmospheric conditions (AM, water vapor, turbidity, albedo, ozone etc.) and computer models were used in generating the global reference spectra in refs. 6 and 7 and the direct reference spectra in refs. 6 and 8, yet they give different calibration numbers at the 1% level. Figure 3 shows a 4% variation in the calibration number for various cell technologies with published AM 0 spectra. In practice, AM 0 reference cells have not been calibrated with respect to a tabular AM 0 spectrum, but have been space flown or balloon flown and calibrated with respect to the extraterrestrial solar spectral irradiance incident on the cell at the time of measurement. Equation (1) gives a method for accurate AM 0 calibration of reference cells without costly space or balloon flights. The use of eqn. (1) for AM 0 calibrations eliminates variations in the calibration number arising from variations in the solar spectral irradiance (sun spots, solar flares etc.).

Once a reference cell has been calibrated with respect to a given reference spectrum, the short-circuit current and hence I–V characteristics can be measured. The measured short-circuit current $I_{sc}^{T,S}$ of the test cell under some light source (the source spectrum) can be corrected for both the spectral mismatch factor M and the intensity using the following expression

$$I_{sc}^{T,R} = \frac{I_{sc}^{T,S}}{M} \frac{I_{sc}^{R,R}}{I_{sc}^{R,S}} \tag{2}$$

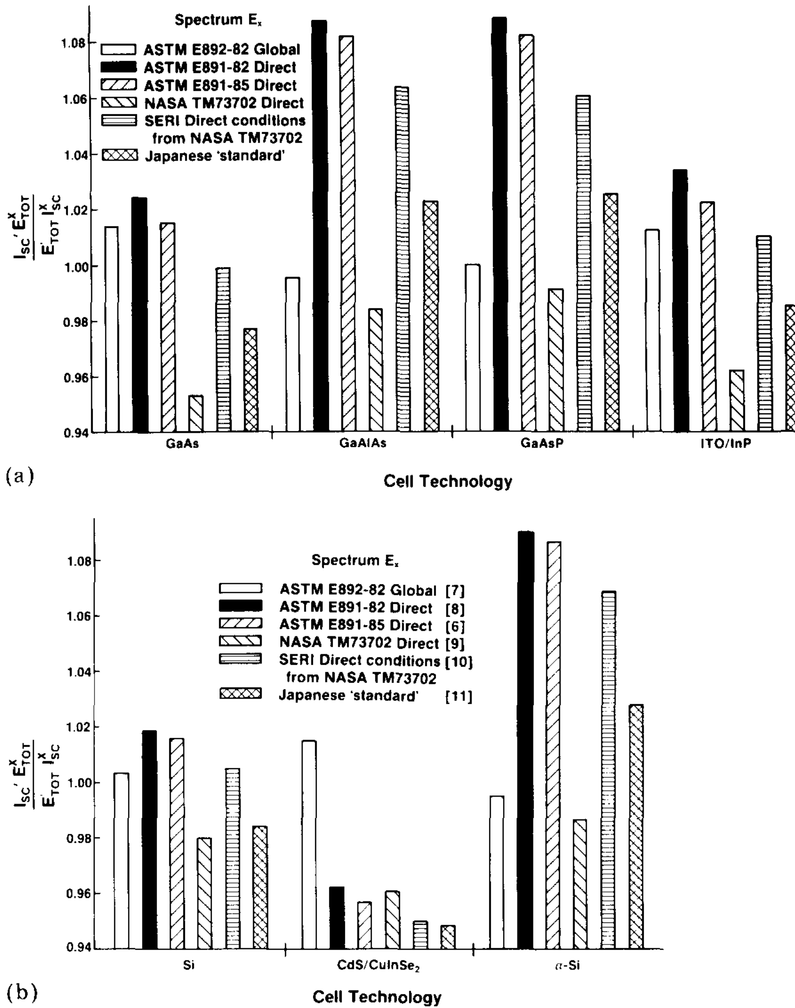

Fig. 2. Comparison of the normalized calibration numbers for various cell technologies and standard AM 1.5 spectra ($E^{x}(\lambda)$, $E_{tot}{}^{x}$, $I_{sc}{}^{x}$) with the ASTM E892 global reference spectrum [6] ($E'(\lambda)$, E_{tot}', I_{sc}').

where $I_{sc}{}^{R,R}$ is the short-circuit current of the reference cell under the reference spectrum (which is the calibration number of the primary reference cell multiplied by 1000 W m^{-2}) and $I_{sc}{}^{R,S}$ is the measured short-circuit current of the reference cell under the source spectrum. Then $I_{sc}{}^{T,R}$ is the short-circuit current of the test cell under the reference spectrum, *i.e.* the measured short-circuit current corrected for both spectral mismatch and intensity. The fractional error, known as the spectral mismatch factor M (introduced because the reference cell spectral response $SR_R(\lambda)$ differs from the spectral response $SR_T(\lambda)$ of the device under test, and the source spectral irradiance $E_S(\lambda)$ differs from the reference spectral irradiance $E_R(\lambda)$) can be computed as follows [3, 16, 17]:

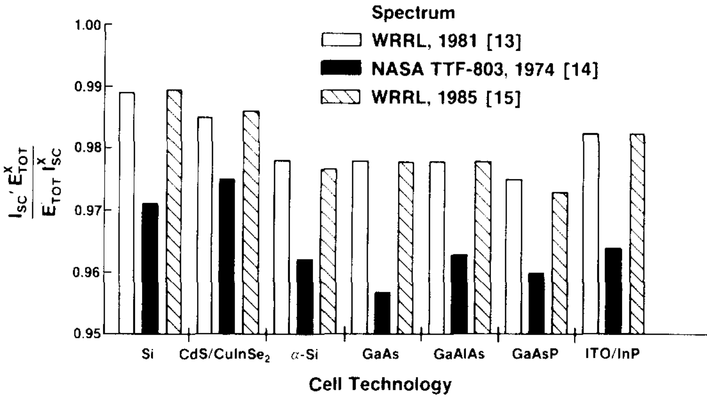

Fig. 3. Comparison of the same cell technologies in Fig. 2 for various AM 0 spectra with the ASTM E490-74 AM 0 spectrum [12].

$$M = \frac{\int_{0.3\,\mu\mathrm{m}}^{4\,\mu\mathrm{m}} E_{\mathrm{R}}(\lambda)\mathrm{SR}_{\mathrm{R}}(\lambda)\,\mathrm{d}\lambda}{\int_{0.3\,\mu\mathrm{m}}^{4\,\mu\mathrm{m}} E_{\mathrm{S}}(\lambda)\mathrm{SR}_{\mathrm{R}}(\lambda)\,\mathrm{d}\lambda} \; \frac{\int_{0.3\,\mu\mathrm{m}}^{4\,\mu\mathrm{m}} E_{\mathrm{S}}(\lambda)\mathrm{SR}_{\mathrm{T}}(\lambda)\,\mathrm{d}\lambda}{\int_{0.3\,\mu\mathrm{m}}^{4\,\mu\mathrm{m}} E_{\mathrm{R}}(\lambda)\mathrm{SR}_{\mathrm{T}}(\lambda)\,\mathrm{d}\lambda} \tag{3}$$

Many investigators assume that M is unity for their particular test cell, reference cell, light source and reference spectrum, which will lead to an error in $I_{sc}^{T,R}$ and hence in the efficiency. For some thin film technologies such as amorphous silicon, the spectral response will be a function of the voltage and, for tandem cells, the spectral response will be a function of the source spectrum. This results in the assumption that, if $I_{sc}^{T,R}$ is correct, then the value of P_{max} should be invalid.

The efficiency of modules is often evaluated at a nominal operating cell temperature (NOCT) instead of at a fixed temperature [18]. The NOCT is the module temperature at a total irradiance of 800 W m^{-2}, a wind velocity of 1 m s^{-1} and an air temperature of 20 °C. The module performance may be corrected to a standard reference spectrum and intensity or may be evaluated under the prevailing outdoor test conditions.

The measurement of the illuminated I–V characteristics under concentrated light is complicated by the measurement of the incident power and non-uniform illumination of the sample. The assumption that the calibration number of the reference cell is a linear function of intensity is no longer valid. The increase in calibration number with intensity has been documented by the use of calibrated neutral density filters [19, 20] to reduce the intensity incident on the reference cell to near 1000 W m^{-2}. The wavelength dependence of the neutral density filters and the variation in the test cell's spectral response with light intensity [10] have not been included in eqns. (2) and (3), and M has usually been assumed to be unity.

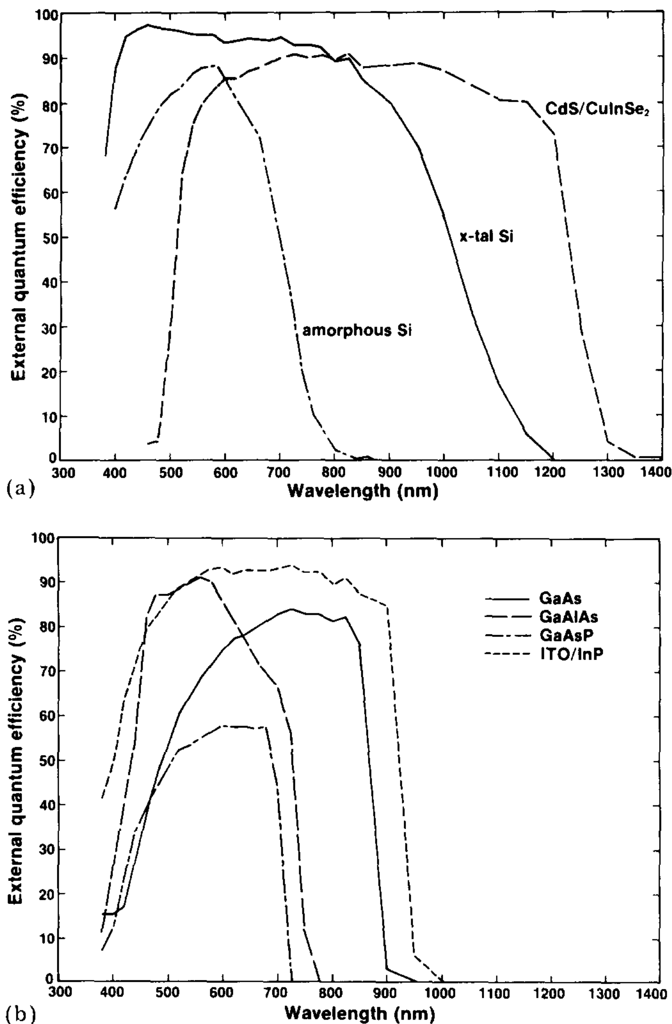

Fig. 4. Measured external quantum efficiencies for the state-of-the-art cells compared in Figs. 2 and 3.

This will result in errors in the short-circuit current and in the efficiency. The magnitude of these errors has not been evaluated but is probably less than the error introduced by assuming that the short-circuit current varies linearly with the intensity. A non-uniform illumination of the test device will reduce the efficiency, and the voltage reduction in a non-uniformly illuminated cell increases with intensity [21].

2.2. Energy rating methods

As PV technologies other than those using crystalline silicon are being evaluated, differences in the sensitivity to variations in the solar spectral irradiance and temperature become more important. The a.m.–p.m. energy

rating method was proposed [22] to account for the wide range of sensitivities among the various PV technologies being considered. This method involves measuring the energy output with respect to a standard day defined by a temperature distribution (15 - 25 °C), 30° latitude and irradiance distribution *vs.* time of day (4.8 kW h m^{-2} horizontal; 5.3 kW h m^{-2} module normal). The spectral irradiance distribution and wind speed are not specified. Translation equations have been developed to allow the energy output to be predicted by an a.m.–p.m. type of scheme given the spectral response, temperature coefficients, NOCT and peak power or efficiency with respect to standard test conditions, and the fill factor *vs.* intensity.

2.3. Current–voltage artifacts

Even if V_{oc}, I_{sc}, FF and η are measured with respect to a set of standard reporting conditions, substantial differences can be encountered. These differences can arise because of hysteresis, light soaking and contacting.

Hysteresis is present when the *I–V* characteristics are not measured in a steady state. The major change occurs near P_{max}, but V_{oc} can also be affected. Figure 5 shows an example of hysteresis for a single-crystal silicon cell [23]. The solution to the problem is to reduce the rate of voltage bias or to measure the current at a fixed voltage.

The *I–V* characteristics for $CdS/CuInSe_2$ solar cells are a reversible function of light exposure time, as shown in Table 2. This phenomenon has been observed in $CdS/CuInSe_2$ thin film cells from a variety of groups, processed in a variety of ways. It appears as if the voltage is the only parameter that is changing with light exposure time. If the cell is biased to I_{sc} for some period of time during light exposure, then the V_{oc}, FF and η will be reduced and rise again asymptotically to a steady state value. Similar variations in V_{oc} with time have been observed for CdS/CdTe, CdS/Cu_2S and ITO/InP cell structures (where ITO is indium tin oxide).

A PV device is an inherently two-terminal device. However, because the *I–V* characteristics of a PV device are dependent on the series resistance

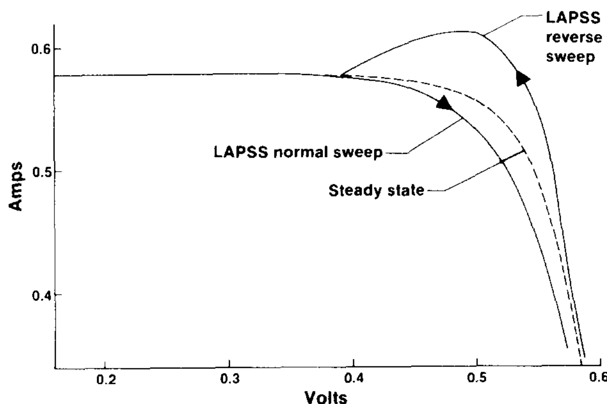

Fig. 5. Single-crystal silicon back surface field solar cell showing hysteresis [23].

TABLE 2

A $CdS/CuInSe_2$ cell showing light soaking, tested at 1000 W m^{-2} and 25 °C (ASTM E892-85 global spectrum)

	Initial exposure to light	*After 2 h 40 min light at V_{oc}*
V_{oc} (V)	0.4023	0.4103
I_{sc} (mA)	26.89	26.88
FF (%)	61.17	62.55
Efficiency (%)	6.6	6.9

V_{oc} (mV) = 410.4 − 1.782 exp{− 0.0273 × time(min)}.

of the device, it is desirable not to add any series resistance with the connections to the measurement system. This source of error can be eliminated with four-terminal contacts to the device which consist of a voltage and a current connection to each terminal. However, care must be taken to place the current and voltage probes as close as possible to each other. This ensures that the voltage measured is the terminal voltage of the device. If one begins to separate the two, as along a top contact bus bar, an increase in fill factor will be observed. The fill factor will reach a maximum when the voltage contact is as far from the current contact as possible along the metallization (including grid lines). Table 3 shows an example of a 100% change in efficiency with different contacting schemes. The resistance between the voltage and current contacts was less than 1 Ω for all four cases. If the resistance between the voltage and current contacts is too high (over 10 Ω), then fill factors approaching unity can be achieved. The number of current contacts or the location of the contacts have not been standardized. Thin film structures are sometimes enhanced by bordering the cell with silver paste and making the devices long and narrow (*i.e.* silver paste on tin oxide for amorphous silicon). This results in an artificial boost in the efficiency, since the silver paste area is not included in the cell area.

TABLE 3

Effect of contacting on light current–voltage characteristics for a polycrystalline silicon cell of area 25 cm^2

J_{sc} (mA cm^{-2})	FF (%)	η (%)	*Contact configuration*	
			Front	*Back*
23.8	37.9	5.4	Kelvin	Common
24.3	64.8	9.4	Kelvin	Kelvin
24.3	69.3	10.0	Kelvin, three current contacts	Kelvin
24.4	74.4	10.8	Separated I and V	Kelvin

Reference conditions: ASTM-85 global, 25 °C, 1000 W m^{-2} with V_{oc} = 0.595 V in all four cases.

3. Instrumentation

There is a wide variety of instrumentation in use by the PV community to measure the efficiency and other *I–V* parameters of a solar cell, module or array. The cost, volume of measurements, speed, repeatability, accuracy, versatility, ease of use and maintenance of a test system are all factors which must be considered. If the system is required to test cells on a production line, then speed and ease of use are major factors. If the system is to be used as a research tool to investigate the *I–V* characteristics of a wide variety of devices, then the repeatability and a wide range of current and voltage is important.

3.1. Current–voltage systems

The basic *I–V* system consists of a variable load, voltmeter, current meter, light source and intensity monitor. The variable load consists of a voltage ramp, variable power supply or load resistors. The use of a voltage ramp is most convenient because, once the ramp rate, initial and final voltages are set, the *I–V* measurement can be initiated by pressing a single button. A variable power supply can be useful in rapidly measuring I_{sc}, P_{max} or the current at a given voltage.

The current through the cell is monitored with a shunt resistor, electrometer or a clamp-on d.c. probe. A shunt resistor is the most common method of measuring the current and uses a voltmeter, *X–Y* recorder, or analog-to-digital (A/D) converter to measure the voltage across the shunt. Most *I–V* systems use a four-terminal shunt resistor. If a two-terminal resistor is used, then the voltage sense wires should be connected, as close as possible, to the resistor and the resistance measured with a four-terminal ohmmeter. It should be noted that any error in the value of the resistance translates directly into an error in the measured current. The power rating on the shunt resistor should be much larger than the product of the square of the maximum current that the system is designed to handle and the value of the shunt resistor. This will prevent errors from being introduced by the resistor heating. The temperature coefficient of the resistor should be as low as possible to prevent errors arising from different ambient temperatures. The value of the shunt resistor should be chosen so that the voltage across the shunt is less than or equal to 100 mV. This will allow the voltage across the variable load to remain close to the voltage across the cell, making the power supply bias and current range less critical. If the voltage across the shunt resistor is low, then resistor noise can become significant and introduce errors in the current that is actually flowing through the cell. The choice of a voltmeter, *X–Y* recorder or A/D converter to measure the voltage across the shunt resistor is dependent on the resolution, accuracy and speed desired. A voltmeter is the most accurate and an *X–Y* recorder is the least accurate, but an A/D converter is the fastest means of measuring the voltage. The use of an electrometer is warranted if the system is required to measure currents below 10 μA. Several investigators have used a clamp-on

d.c. probe because it is easy to use and does not load the circuit. The use of a d.c. probe is limited to a narrow current range and may give misleading values if not used properly.

The voltage across the cell is easily measured with any high impedance voltmeter or X–Y recorder. The limiting uncertainty in the voltage measurement is the ability to monitor and control the junction temperature accurately. Near the maximum power point, uncertainties in the voltage can arise from the contacting method.

The measurement of the maximum power P_{max} can be performed manually by monitoring the product of the voltage and the current. Constant power curves overlayed on an I–V plot produced by an X–Y recorder can also be used, or the I–V curve can be digitized near the maximum power point to determine the voltage and current at P_{max}. These graphical methods are limited by the width of the line producing the I–V curve and the operator's ability to set the zero and to determine P_{max}. Analog circuits have been developed to track the maximum power point of cells, modules or arrays. Although the accuracy of these circuits is limited by their ability to home in on P_{max} in the presence of fluctuations in the current, these circuits can usually locate P_{max} to within 10 mV, which is acceptable for arrays or modules but may not be acceptable for devices. The cheapest and most accurate method of measuring P_{max} is to use an X–Y recorder to obtain the fill factor, a voltmeter to obtain V_{oc} under open-circuit conditions and a voltmeter with a four-terminal shunt resistor to obtain I_{sc}.

There is a wide variety of instrumentation available to measure the I–V characteristics of a device which include several curve tracers suitable for evaluating solar cells. The I–V curve is displayed on a cathode ray tube or digital display and the I–V characteristics are available as analog outputs or from the IEEE-488 (HPIB) or other computer interfaces. The use of resistive loads to evaluate the I–V characteristics of modules or arrays is common because resistor arrays can dissipate large amounts of power and provide a convenient means for stability studies near P_{max} or I_{sc}.

Commercially available efficiency measurement systems have a wide variety of features including the determination of V_{oc}, I_{sc} and P_{max} in addition to providing analog outputs for an X–Y recorder or voltmeter, but they are usually incapable of measuring illuminated I–V characteristics in reverse bias.

I–V systems based on a capacitive charging scheme that are compact, require little power and can evaluate up to 10 kW arrays have been developed [24]. The concept is based on the charging of a capacitor by an array which will sweep the I–V curve from I_{sc} to V_{oc} over a period of about 1 s. The data are analyzed using high speed A/D converters, timing circuitry and a microprocessor. A power supply is used to apply an initial reverse bias to the array.

There are several hybrid units on the market built around a specific solar simulator allowing production-oriented testing. Many investigators use curve tracers to evaluate the illuminated and dark I–V characteristics of a

device. This technique is useful in rapidly measuring the I–V properties of a device but is limited by the ability to read the voltage and current accurately from the curve. Curve tracers can also easily damage a cell by overbiasing if the operator is not careful.

A wide variety of automated I–V test systems have been built to suit a range of needs. Several papers have been published describing automated I–V measurements [4, 25 - 28]. These systems are characterized by a D/A converter to replace the variable load and utilize A/D conversion to monitor the voltage across the cell and the shunt resistor. Automated systems offer graphical and tabular presentation of the data in addition to database management and numerical analysis of the data. Automated test systems are also capable of correcting the illuminated current for fluctuations in the light intensity about a set value which can achieve better than $\pm 0.05\%$ repeatability in the current with $\pm 1\%$ intensity fluctuations, a capability which manual I–V systems do not have. Automated systems can also employ averaging and search algorithms to improve the precision of V_{oc}, I_{sc} and P_{max}.

3.2. Spectral response

The spectral response of a solar cell or module is a valuable diagnostic tool and is essential in calibrating reference cells (eqn. (1)) and performing spectral mismatch calculations (eqn. (3)). A review of spectral response measurement instrumentation and techniques is given in refs. 29 - 31. A simplified spectral response measurement apparatus consists of a light source, collimating optics, light chopper and a filter wheel or grating monochromator giving narrow band monochromatic light incident on a sample. The photocurrent is measured with a current-to-voltage converter and lock-in amplifier or true-r.m.s. voltmeter. The photocurrent is normally measured at zero voltage bias and a light bias of 1000 W m^{-2}. The photocurrent divided by the incident monochromatic light intensity is the spectral response in units of ampères per watt, and the quantum efficiency in units

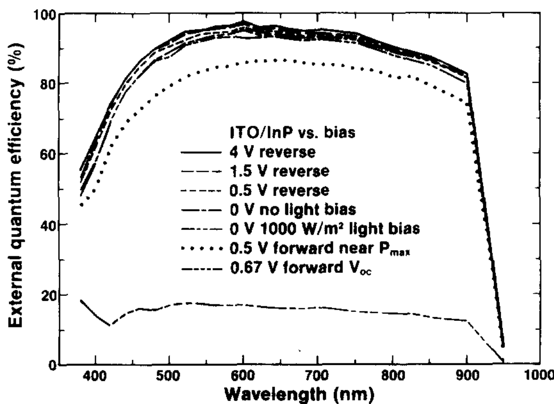

Fig. 6. Effect of bias voltage on the quantum efficiency of an ITO/InP solar cell.

of electrons per photon is simply the spectral response divided by the electronic charge and the wavelength and multiplied by Planck's constant and the speed of light. The monochromatic light intensity incident on the cell is usually measured with a calibrated silicon photodiode or spectrally flat pyroelectric radiometer. The spectral response is a function of the bias light intensity [20, 31, 32] and voltage bias. The spectral response of multijunction solar cells is a function of voltage bias, and the intensity and spectral content of the bias light [33]. The effect of voltage bias on the quantum efficiency of an ITO/InP solar cell is shown in Fig. 6. Using the GaAs cell in Fig. 4(b) as the reference cell, the global reference spectrum in ref. 6 and the Spectrolab X-25 spectral irradiance in ref. 5, the spectral mismatch index M (eqn. (3)) varied from 0.989 to 0.999.

This shows that, for a reasonably well-matched reference cell and solar simulator, the error introduced by the voltage dependence of the spectral response is negligible (about $\pm 1\%$). This may not be true when the relative spectral response is a strong function of voltage or light bias such as is the case for amorphous silicon or multijunction solar cells.

4. Conclusions

A wide variety of information can be obtained from measuring the current as a function of voltage, temperature, intensity and spectrum. A brief overview of illuminated $I-V$ measurements of PV devices has been presented. The use of the terms AM 1.5 and AM 0, 1 Sun or other abbreviated descriptions of standard reporting conditions for the efficiency is ambiguous and should be avoided. Large differences in the efficiency can and do occur because of non-standard measurement techniques and definitions. The instrumentation required for accurate $I-V$ or spectral response measurements is readily available. The ability to measure the efficiency with respect to standard reporting conditions is more difficult, since various temperature, spectral and intensity translation equations are required. The measurement of the efficiency for a cell under concentration with respect to standard reporting conditions is complicated by the difficulty in measuring the temperature of the cell and the spectral irradiance incident on the cell. The use of an energy rating method to evaluate the performance of a PV technology eliminates many of the translation equations and allows the performance to be evaluated in the context of its intended application. The major drawback of an energy rating method is that it is location specific and impractical for unencapsulated research-type devices.

Acknowledgment

This work was supported by the U.S. Department of Energy under Contract DE-AC02-83CH10093.

References

1 L. J. Reiter, C. S. Borden, J. L. Smith and L. W. Zimmerman, *Rating Methods for Flat-Plate and Concentrator Photovoltaic Modules and Systems, JPL Rep. D-1805*, October 1984 (Jet Propulsion Laboratory, Pasadena, CA).
2 K. A. Emery, *Sol. Cells, 18* (1986) 251 - 260.
3 C. R. Osterwald, *Sol. Cells, 18* (1986) 269 - 279.
4 K. A. Emery and C. R. Osterwald, *Sol. Cells, 17* (1986) 253 - 274.
5 K. A. Emery, C. R. Osterwald, T. W. Cannon, D. R. Myers, J. Burdick, T. Glatfelter, W. Czubatyj and J. Yang, *Proc. 18th IEEE Photovoltaic Specialists' Conf., Las Vegas, NV, October 21 - 25, 1985*, IEEE, New York, 1986, pp. 623 - 628.
6 R. Hulstrom, R. Bird and C. Riordan, *Sol. Cells, 15* (1985) 365 - 391; *ASTM Stand. E891, ASTM Stand. E892*, 1987 (ASTM, Philadelphia, PA).
7 *Terrestrial Solar Spectral Irradiance Tables at Air Mass 1.5 for a 37° Tilted Surface, ASTM Stand. E892, 1982* (ASTM, Philadelphia, PA).
8 *Terrestrial Direct Normal Solar Spectral Irradiance Tables for Air Mass 1.5, ASTM Stand. E891*, 1982 (ASTM, Philadelphia, PA).
9 *Terrestrial Photovoltaics Measurement Procedures, NASA Tech. Memo. TM 73702*, 1977 (National Aeronautics and Space Administration, Cleveland, OH).
10 C. R. Osterwald, T. W. Cannon and D. R. Meyers, *Proc. SERI Photovoltaic Advanced Research and Development Projects, Golden, CO, October 29 - 31, 1984*, in *Rep. SERI/CP-211-2507* (Solar Energy Research Institute, Golden, CO) (see ref. 4 for table).
11 R. Shimokawa, K. Fujisaw, M. Horiguchi, S. Yoshikawa and Y. Hamakawa, *Proc. 5th Commission of the European Communities Conf. on Photovoltaic Solar Energy, Athens, Greece, October 17 - 21, 1983*, Reidel, Dordrecht, 1983, pp. 657 - 661.
12 *Standard Solar Constant and Air Mass Zero Solar Spectral Irradiance Tables, ASTM Stand. E490*, 1973 (ASTM, Philadelphia, PA).
13 Spectrum revised and extended by the work of H. Neckel and D. Labs, Improved data of solar spectral irradiance from 0.33 μm to 1.25 μm, *Sol. Phys., 74* (1) (1981) 231 - 249 (provided by C. D. Frohlich and C. Wehrli, World Radiation Centre, Davos-Dorf, Switzerland).
14 Y. A. Makarova and A. V. Kharitonov, *Distribution of Energy in the Solar Spectrum and the Solar Constant, NASA Tech. Memo. TT F-803*, 1974 (available from National Technical Information Service, Springfield, VA).
15 C. Wehrili, *Extraterrestrial Solar Spectrum, Publ. 615*, July 1985 (Physikalisch-Meteorologisches Observatorium and World Radiation Center, Davos-Dorf, Switzerland).
16 *Standard Practice for Determination of the Spectral Mismatch Parameter Between Photovoltaic Devices and Photovoltaic Reference Cell, ASTM Stand. E973*, 1983 (ASTM, Philadelphia, PA).
17 C. H. Seaman, *Sol. Energy, 29* (1982) 291.
18 R. G. Ross, *Sol. Cells, 18* (1986) 345 - 352.
19 R. W. Sanderson, J. D. Birkeland, S. C. Martin and C. E. Backus, *Proc. 17th IEEE Photovoltaic Specialists' Conf., Kissimmee, FL, May 1 - 4, 1984*, IEEE, New York, 1984, pp. 1309 - 1313.
20 R. W. Sanderson, C. E. Backus and J. Birkeland, *Proc. 16th IEEE Photovoltaic Specialists' Conf., San Diego, CA, September 27 - 30, 1982*, IEEE, New York, 1983, pp. 454 - 458.
21 S. R. Dhariwal, R. K. Mathar and R. Gadre, *J. Phys. D, 14* (1981) 1325.
22 C. F. Gay, J. E. Rumburg and J. H. Wilson, *Proc. 16th IEEE Photovoltaic Specialists' Conf., San Diego, CA, September 27 - 30, 1982*, IEEE, New York, 1983, pp. 1041 - 1046.
23 J. Lovelady, personal communication, *Large Area Pulsed Solar Simulator Testing of Back Surface Field Solar Panels, Internal Rep.*, 1985 (Spectrolab Inc., Sylmar, CA).
24 T. H. Warner and C. H. Cox, *Sol. Cells, 7* (1982) 175.

25 R. Schultz, *IEEE Trans. Inst. Meas.*, *26* (1976) 295.
26 L. Castaner, *IEEE Trans. Inst. Meas.*, *27* (1978) 152.
27 K. Emery and J. DuBow, *Proc. 14th IEEE Photovoltaic Specialists' Conf., San Diego, CA, January 7 - 10, 1980*, IEEE, New York, 1980, pp. 506 - 510.
28 H. Gerwin, *Photovoltaic Advanced Systems Test Facility: Description and Operations Plan, Rep. SAND 80-1612*, 1980 (Sandia Laboratories, Albuquerque, NM).
29 J. S. Hartman and M. A. Lind, *Sol. Cells*, *7* (1982) 147.
30 *Standard Methods for Measuring the Spectral Response of Photovoltaic Cells, ASTM Stand. E1021*, 1984 (ASTM, Philadelphia, PA).
31 E. F. Zalewski and J. Geist, *Appl. Opt.*, *18* (1979) 3942.
32 V. Augelli, L. Vasanelli, M. Leo, R. A. Leo and G. Soliani, *J. Appl. Phys.*, *53* (1982) 1558.
33 G. F. Virshup, *Proc. 18th IEEE Photovoltaic Specialists' Conf., Las Vegas, NV, October 21 - 25, 1985*, IEEE, New York, 1986, pp. 618 - 622.